Roughness-Facilitated Local 1/2 Scaling Does Not Imply the Onset of the Ultimate Regime of Thermal Convection

Xiaojue Zhu,[1,*] Richard J. A. M. Stevens,[1] Roberto Verzicco,[2,1] and Detlef Lohse[1,3,†]
[1]Physics of Fluids Group and Max Planck Center Twente, MESA+ Institute and J. M. Burgers Centre for Fluid Dynamics, University of Twente, P.O. Box 217, 7500AE Enschede, Netherlands
[2]Dipartimento di Ingegneria Industriale, University of Rome "Tor Vergata," Via del Politecnico 1, Roma 00133, Italy
[3]Max Planck Institute for Dynamics and Self-Organization, 37077 Göttingen, Germany
(Received 27 March 2017; published 11 October 2017)

In thermal convection, roughness is often used as a means to enhance heat transport, expressed in Nusselt number. Yet there is no consensus on whether the Nusselt vs Rayleigh number scaling exponent ($\mathrm{Nu} \sim \mathrm{Ra}^{\beta}$) increases or remains unchanged. Here we numerically investigate turbulent Rayleigh-Bénard convection over rough plates in two dimensions, up to $\mathrm{Ra} \approx 10^{12}$. Varying the height and wavelength of the roughness elements with over 200 combinations, we reveal the existence of two universal regimes. In the first regime, the local effective scaling exponent can reach up to 1/2. However, this cannot be explained as the attainment of the so-called ultimate regime as suggested in previous studies, because a further increase in Ra leads to the second regime, in which the scaling saturates back to a value close to the smooth wall case. Counterintuitively, the transition from the first to the second regime corresponds to the competition between bulk and boundary layer flow: from the bulk-dominated regime back to the classical boundary-layer-controlled regime. Our study demonstrates that the *local* 1/2 scaling does not necessarily signal the onset of ultimate turbulence.

DOI: 10.1103/PhysRevLett.119.154501

Thermal convection plays an important role in a wide range of natural and industrial environments and settings. The paradigmatic representation of thermal convection, Rayleigh-Bénard (RB) flow, in which a fluid is heated from below and cooled from above, has received extensive attention over the past decades [1–3]. One of the major challenges in the studies of RB convection is to determine the scaling relation of the Nusselt number (Nu), which is the dimensionless heat flux, with the Rayleigh number (Ra), which is the dimensionless temperature difference between the two plates, expressed as $\mathrm{Nu} \sim \mathrm{Ra}^{\beta}$.

From similarity theory, Priestley [4] argued that $\beta = 1/3$. Assuming that the heat transport is independent of the cell height and governed by the viscous boundary layers (BL), Malkus [5] also derived that $\beta = 1/3$. Later, Grossmann and Lohse [6,7] showed that there is no pure scaling but smooth transitions from BL to bulk dominated regimes. However, for large Ra when the BLs have become turbulent, Kraichnan [8] postulated that the flow reaches the so-called ultimate regime, in which Nu scales according to $\mathrm{Nu} \sim \mathrm{Ra}^{1/2}(\ln \mathrm{Ra})^{-3/2}$, with $(\ln \mathrm{Ra})^{-3/2}$ as the logarithmic correction term. This ultimate regime was also predicted by Grossmann and Lohse [9], who modeled this logarithmic behavior with an effective scaling exponent of $\beta \approx 0.38$, for Ra around 10^{14}. Experimentally, for $\mathrm{Ra} \approx 10^{14}$ the onset of such a regime has been observed [10,11]. The logarithmic correction term has minor impact for very large Ra. In the asymptotic ultimate regime $\beta = 1/2$, and the heat transport is independent of viscosity and therefore the scaling can be extrapolated to arbitrarily large Ra, as suggested for both geophysical and astrophysical flows. This asymptotic ultimate 1/2 scaling has numerically [12,13] and experimentally [14,15] been observed in the so-called "homogeneous" or "cavity" RB turbulence, where no BLs are present.

Clearly, the interplay between BL and bulk flow determines the effective scaling exponent [6]. To better understand the role of the BLs, it is important to alter the boundaries to probe how the system responds. Hence, much attention has been paid to RB turbulence over rough surfaces. Another motivation is the fact that the underlying surfaces of real-world applications of thermal convection are always rough. It is generally agreed that roughness enhances the absolute value of Nu. However, it has been reported that the *scaling exponent* increases with roughness [16–25] or remains unchanged [26–28] as compared to the smooth counterpart, depending on the range of Ra explored and the roughness configurations. For example, Shen *et al.* [26] found that Nu increased by 20%, whereas the exponent β did not change upon using rough surfaces made of regularly spaced pyramids. Roche *et al.* [18] obtained an increase of β to approximately 0.51 by implementing V-shaped axis-symmetrical grooves both on the sidewalls and horizontal plates. Very recently, simulations of RB with rough walls were done in the range $\mathrm{Ra} = [4 \times 10^6, 3 \times 10^9]$ and a roughness induced effective 1/2 scaling was found in the range $\mathrm{Ra} = [10^8, 3 \times 10^9]$. This was explained as the attainment of the ultimate regime [24]. However, it is surprising that the ultimate regime can be found at such low Ra since theories predict that the ultimate regime 1/2 scaling can

only be observed asymptotically when the BLs are highly turbulent [9].

In this study, we will unify these different views. For this, we perform direct numerical simulations (DNS) of turbulent RB convection over sinusoidally rough plates in two dimensions (2D), adopting the same roughness configuration as in Ref. [24]. The effects of roughness on heat transport are presented by varying the heights h and wavelengths λ of the rough elements independently. We note that, for the smooth case, 2D RB differs from three dimensional (3D) RB in terms of (a) integral quantities for finite Pr [29,30], (b) scaling arguments (the asymptotic exponent β is $1/2$ in 3D [31,32], but $5/12$ in 2D [33]), and (c) BL stability [34]. However, for the rough case, 2D and 3D have the same aysmptotic scaling exponent $1/2$ [35]. Moreover, 2D simulations are much less time consuming than 3D and can help us push forward to $\mathrm{Ra} \approx 10^{12}$ and $\mathrm{Nu} \sim \mathcal{O}(10^3)$ with roughness. This key extension to large Ra unravels the physical origin of the $1/2$ regimes observed in Ref. [24].

The simulations were performed using a second-order finite-difference code [36,37], in combination with an immersed-boundary method [38] to track the rough elements. No-slip conditions were used for the velocity, constant temperature boundary conditions for rough bottom and top plates, and periodic boundary conditions for the horizontal sidewalls. The control parameters are $\mathrm{Ra} = \alpha g \Delta (L-h)^3/(\nu\kappa)$ and the Prandtl number $\mathrm{Pr} = \nu/\kappa$, where α is the thermal expansion coefficient, g the gravitational acceleration, Δ the temperature difference between the two plates, L the height of the domain without roughness, h the height of the roughness element, ν the kinematic viscosity, and κ the thermal diffusivity. The reason to choose $L-h$ for the rough cases as the characteristic length is that it resembles the height between the two smooth plates where the same volume of fluid occupies. The other flow quantities are nondimensionalized by the temperature difference Δ and the free fall velocity $U = \sqrt{\alpha g \Delta (L-h)}$. In all simulations, $\mathrm{Pr} = 1$ and the aspect ratio $\Gamma = D/L = 2$, where D is the width of the domain. With this Γ, the heat flux approximates the heat flux at an infinite aspect ratio [39]. Three roughness heights were chosen, $h/L = 0.05$, 0.1, and 0.15. For each height, the wavelength of roughness λ/L was varied from 0.05 to 0.7. For each combination of wavelength and height, we performed simulations in the range of $\mathrm{Ra} = [10^8, 10^{12}]$. Adequate resolution was ensured for all cases and the statistics were averaged over 200 free fall time units. At $\mathrm{Ra} = 7.3 \times 10^{11}$ with $\lambda = h = 0.1L$, $14\,336 \times 7168$ grid points were used. Nu is calculated from $\mathrm{Nu} = \sqrt{\mathrm{Ra}\,\mathrm{Pr}}\langle u_z\theta\rangle_A - \langle \partial_z\theta\rangle_A$, where u_z denotes the vertical velocity, θ the temperature, and $\langle\cdots\rangle_A$ the average over time and any horizontal plane.

We begin by comparing the temperature field with increasing Ra (see Fig. 1), for a fixed set of roughness parameters ($\lambda/L = 0.1$ and $h/L = 0.1$). Here we stress the plume morphology inside the cavity regions between the rough elements. For the two smaller $\mathrm{Ra} = 2.2 \times 10^8$ and $\mathrm{Ra} = 2.2 \times 10^9$, thermal plumes are mainly generated from the tips of the rough elements and are detached towards the directions of the large scale rolls, while in the cavity regions the flow is viscosity dominated. Note that below $\mathrm{Ra} = 2.2 \times 10^8$, roughness elements are submerged inside the thermal boundary layer. In comparison, at $\mathrm{Ra} = 7.3 \times 10^{11}$, plumes are not only generated at the tips but also at the sloping surfaces of the rough elements. Inside the cavities, the detached plumes mix the fluid vigorously, making the flow there more turbulent. These observations suggest that even after the rough elements protrude beyond the thermal BL, the flow structure is essentially similar for one decade of Ra while it changes drastically when further increasing Ra so that the flow inside the cavities becomes turbulent.

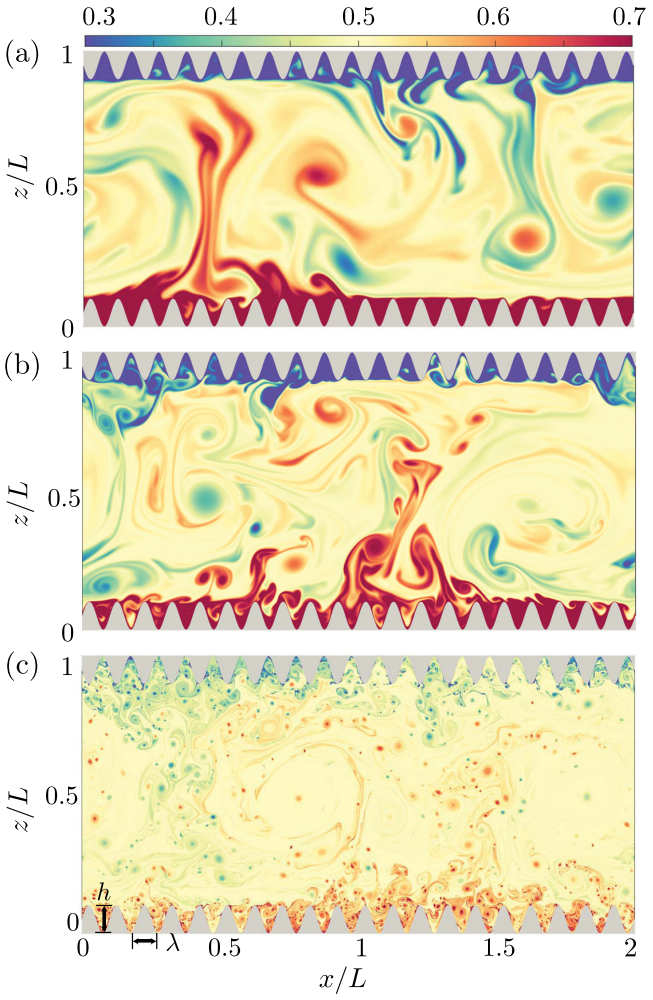

FIG. 1. The instantaneous temperature fields for $\lambda/L = 0.10$ and $h/L = 0.10$ at (a) $\mathrm{Ra} = 2.2 \times 10^8$, (b) $\mathrm{Ra} = 2.2 \times 10^9$, and (c) $\mathrm{Ra} = 7.3 \times 10^{11}$, where λ is the wavelength and h the height of the roughness. The three plots share the same color map.

We now systematically explore the heat transport as a function of Ra, covering more than four decades. The

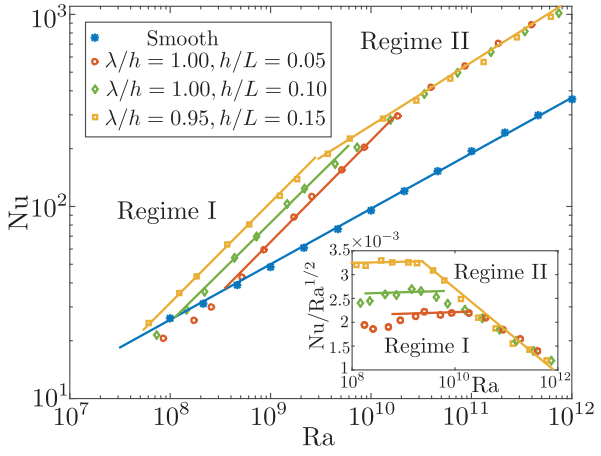

FIG. 2. Nu(Ra) for rough cases of aspect ratio $\lambda/h \approx 1$ at $h/L = 0.05$, 0.10 and 0.15, in comparison to the smooth case, for which the scaling exponent is $\beta = 0.29 \pm 0.01$. For the rough cases, two regimes can be identified: regime I, $\beta = 0.50 \pm 0.02$ and regime II, $\beta = 0.33 \pm 0.01$. The inset shows the compensated plot and the plateau demonstrates the robustness of $1/2$ scaling in regime I. Clearly, a single power law cannot hold for the whole extent of data.

resulting Nu(Ra) dependences with the same roughness aspect ratio $\lambda/h \approx 1$ for different roughness heights are displayed in Fig. 2. The smooth case follows an effective scaling exponent $\beta = 0.29$, in very good agreement with previous studies [30,40]. With the introduction of roughness, two universal regimes can be identified. When the roughness elements protrude the thermal BL, heat transport is enhanced dramatically and the local effective scaling exponent is close to $1/2$, extending more than one decade, similar to the one obtained previously [24]. We call this regime I, the enhanced exponent regime. This scaling exponent is robust as it does not change when altering the roughness height in the range [0.05, 0.15]. The higher the roughness is, the earlier the system steps into regime I. However, further increasing Ra does not result in an extension of regime I. Instead, the scaling exponent saturates back to the effective value $\beta \approx 0.33$, which is the typical Malkus exponent in the classical regime where the BL is of laminar type [5–7]. We call this regime II, the saturated exponent regime. Remarkably, the heat transport follows exactly the same line in this regime for different roughness height. The heat transfer increases 3.05 times while the wet surface area augment is 2.30 times, suggesting that the heat transfer enhancement is mainly due to the enlarged surface area while strong plume ejections in the cavities contribute the remaining part.

Next, we vary the roughness wavelength λ, focusing on the effective scaling exponent β, up to $\mathrm{Ra} \approx 10^{12}$. A similar approach was employed in Refs. [24,41], and now we extend to the two regimes and different heights of roughness. No matter what λ is, we still identify the regime I where the effective exponent increases and regime II where it saturates back to a value close to 0.33. Figure 3(a) demonstrates the scaling exponents in regime I. For each roughness height, there is always an optimal λ which maximizes the effective scaling exponent to $1/2$. However, for each h, the optimal λ is different. A better parameter to describe the effects of roughness on the scaling exponent is the roughness aspect ratio λ/h, as shown in Figs. 3(b) and 3(c) for regime I and regime II, respectively. Interestingly, all the data collapse into one line and specifically for the optimum we find $\lambda/h \approx 1$, irrespective of the roughness height.

The various studies reported in the literature fall into either of the two regimes we revealed here. Namely, the regime where the effective scaling increases up to $\mathrm{Ra}^{1/2}$ [18,24] or the regime where the scaling is similar [26–28] to the smooth case. These seemingly contradictory viewpoints have caused some confusion in the interpretation of the data on RB convection with roughness. The present study has bridged the gap between the two views by studying a sufficiently large regime in Ra and also various roughness characteristics. The clear conclusion is that the observed local effective $1/2$ scaling in regime I should not be interpreted as the attainment of the so-called ultimate regime as suggested in previous studies [24], but rather as a crossover regime in which the roughness elements start to perturb the thermal BL. Only once the BLs become turbulent does the transition to the ultimate regime really occur [1,9] and the asymptotic $1/2$ scaling might be seen. This provides a consistent and plausible explanation for the

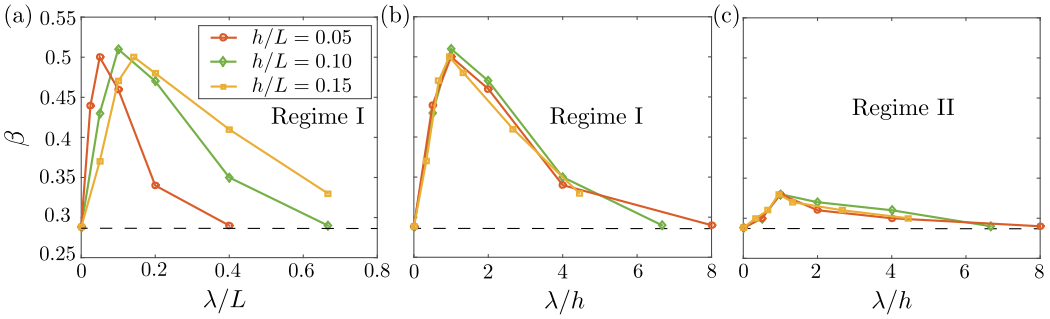

FIG. 3. The Nu vs Ra effective scaling exponents β in regime I and regime II as a function of (a) roughness wavelength λ in regime I, and (b),(c) aspect ratio λ/h in regime I and II, respectively. Note that both $\lambda = 0$ and $\lambda = \infty$ correspond to the smooth plate case (dashed line).

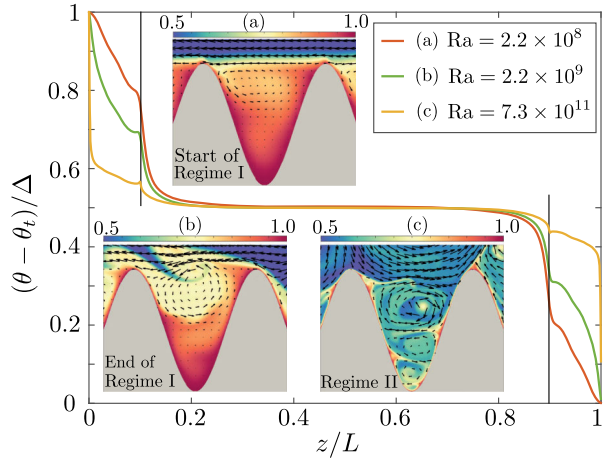

FIG. 4. The dimensionless mean temperature profiles $(\theta - \theta_t)/\Delta$ for $\lambda/h = 1.00$ and $h/L = 0.10$ at (a) the start of regime I ($\mathrm{Ra} = 2.2 \times 10^8$), (b) the end of regime I ($\mathrm{Ra} = 2.2 \times 10^9$), and (c) regime II ($\mathrm{Ra} = 7.3 \times 10^{11}$), where θ_t is the temperature of the top plate. The insets show the temperature fields, superposed by the velocity vectors in the cavity regions. In regime I, one roll is inside the cavity, whereas in regime II, there are multiple. The two black lines indicate where the tips of the roughness elements are.

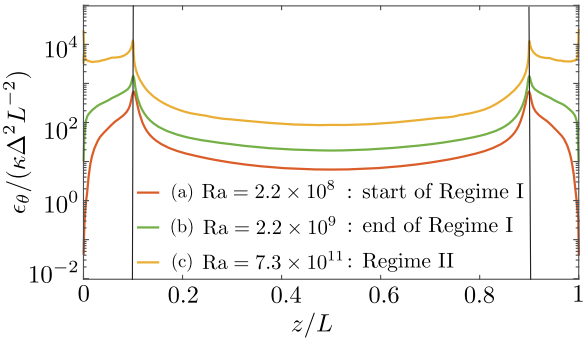

FIG. 5. The dimensionless mean thermal energy dissipation rate $\epsilon_\theta/(\kappa\Delta^2 L^{-2})$ across the height of the domain for $\lambda/h = 1.00$, $h/L = 0.10$ at (a) the start of regime I ($\mathrm{Ra} = 2.2 \times 10^8$), (b) the end of regime I ($\mathrm{Ra} = 2.2 \times 10^9$), and (c) regime II ($\mathrm{Ra} = 7.3 \times 10^{11}$). The two black lines indicate where the tips of the roughness elements are.

observed scatter in the reported values of β with the presence of roughness in prior studies [16,17,19–23], where different combinations of h and λ were chosen. We show that tuning h and λ can lead to big variations of β, especially in regime I (Fig. 3), presumably causing the scattered effective scaling exponents. We note that the optimal $\lambda/h \approx 1$ reported here is different compared to previous studies, namely $\lambda/h \approx 5$ in Ref. [20] and $\lambda/h \approx 0.25$ in Ref. [25]. However, we also note that the roughness shapes and layouts are different among these studies. Only by doing DNS in one-to-one comparisons with these experiments can we ultimately resolve the origins of these differences.

To disentangle the mechanisms leading to the two regimes, in Fig. 4 we show the temperature profiles as well as the local flow structures inside the cavities for $\lambda/h = 1.00$ and $h/L = 0.10$ at different Ra. We observe secondary vortices induced by large scale rolls. In regime I, the weak secondary vortices cannot efficiently mix the fluid in the cavities and thus the flow there is still viscosity dominated. Therefore, the temperature profile in the cavity is rather linear. In regime II, secondary vortices are strong enough to induce smaller vortices, which further induce even smaller vortices down to the centers of the valleys, forming a cascade of vortices. Because of the strong mixing of this process, the roughness elements are covered by a thin thermal BL which is uniformly distributed along the rough surfaces, effectively mimicking an enlarged surface area. As a result, the mean velocity profile is steep only at the center of the valleys and otherwise becomes very similar to the smooth case. The findings here also suggest that for even larger Ra, the scaling exponent in the rough case might finally become the same as in the smooth case.

Inside the cavities, in regime I, the viscosity dominated flow decreases the BL contribution to the total thermal energy dissipation, while in regime II, the restoration of the uniformly distributed BL brings back the BL contribution to the total thermal energy dissipation. For the thermal energy dissipation, it has been well known that if the bulk contribution is dominant, the scaling exponent is close to $1/2$ and if the BL contribution dominates, the scaling exponent is close to $1/3$, i.e., in the classical regime where the BL is of laminar type [6,7]. Here, due to the effective scaling, regime I seems to be the bulk dominated regime whereas regime II seems to be the classical BL-controlled regime. This is counterintuitive since one would expect the opposite with increasing Ra for the smooth RB, i.e. the system becomes more bulk dominated with increasing Ra [6,7,9]. In Fig. 5 we show the mean thermal energy dissipation rate along the height. Indeed, in regime I, the thermal dissipation inside the cavity is negligible, whereas in regime II, the thermal dissipation inside the cavity is dominated, supporting the above interpretation on the reverse role of BL and bulk in the presence of roughness.

In conclusion, the present study has demonstrated that the local effective $\beta = 1/2$ scaling in RB with roughness does not *necessarily* indicate the start of the ultimate regime as claimed in previous studies [24]. Instead, its observation is fortuitous because by tuning the height and wavelength of roughness elements simultaneously, β can be tuned between 0.29 and 0.5 locally. This regime I is just a crossover regime where the bulk is dominated, as has been speculated in Refs. [1,20,25]. Further increasing Ra brings back the thin BL inside the cavities and restores the classical BL-controlled regime, causing the scaling saturation and recovering the classical RB scaling exponent. Only at even higher Ra the real transition to the ultimate scaling might be seen.

Finally, we note that for Taylor-Couette (TC) flow with roughness which aligns with the azimuthal direction,

DNS showed that for the angular velocity transfer scaling $Nu_\omega \sim Ta^\beta$, both regime I where β increases up to $1/2$ and regime II where β saturates back were also observed [42]. Here, Ta is the dimensionless angular velocity difference which plays the equivalent role to Ra in RB. Thus, there is strong evidence that the two systems are not only analogous with each other in the smooth case [11,43–45] but also in the rough case. However, for TC flow with roughness which inhibits the azimuthal flow, this analogy might break down. In that case, the main contribution to the angular velocity transfer originates from the pressure forces rather than the viscous forces. In contrast, in RB, the temperature is a scalar and there is nothing similar to the effects of pressure which could contribute to the heat transfer [46].

We thank V. Mathai for fruitful discussions. This work is supported by FOM and MCEC; both are part of the Netherlands Organisation for Scientific Research (NWO). We thank the Dutch Supercomputing Consortium SURFSara, the Italian supercomputer Marconi-CINECA through the PRACE Project No. 2016143351 and the ARCHER UK National Supercomputing Service through the DECI Project 13DECI0246 for the allocation of computing time.

*xiaojue.zhu@utwente.nl
†d.lohse@utwente.nl

[1] G. Ahlers, S. Grossmann, and D. Lohse, Rev. Mod. Phys. **81**, 503 (2009).
[2] D. Lohse and K.-Q. Xia, Annu. Rev. Fluid Mech. **42**, 335 (2010).
[3] F. Chillà and J. Schumacher, Eur. Phys. J. E **35**, 58 (2012).
[4] C. H. B. Priestley, Aust. J. Phys. **7**, 176 (1954).
[5] M. V. R. Malkus, Proc. R. Soc. A **225**, 196 (1954).
[6] S. Grossmann and D. Lohse, J. Fluid Mech. **407**, 27 (2000).
[7] S. Grossmann and D. Lohse, Phys. Rev. Lett. **86**, 3316 (2001).
[8] R. H. Kraichnan, Phys. Fluids **5**, 1374 (1962).
[9] S. Grossmann and D. Lohse, Phys. Fluids **23**, 045108 (2011).
[10] X. He, D. Funfschilling, E. Bodenschatz, and G. Ahlers, New J. Phys. **14**, 063030 (2012).
[11] X. He, D. Funfschilling, H. Nobach, E. Bodenschatz, and G. Ahlers, Phys. Rev. Lett. **108**, 024502 (2012).
[12] D. Lohse and F. Toschi, Phys. Rev. Lett. **90**, 034502 (2003).
[13] E. Calzavarini, D. Lohse, F. Toschi, and R. Tripiccione, Phys. Fluids **17**, 055107 (2005).
[14] M. Gibert, H. Pabiou, F. Chilla, and B. Castaing, Phys. Rev. Lett. **96**, 084501 (2006).
[15] S. S. Pawar and J. H. Arakeri, Phys. Rev. Fluids **1**, 042401 (2016).
[16] S. Ciliberto and C. Laroche, Phys. Rev. Lett. **82**, 3998 (1999).
[17] G. Stringano, G. Pascazio, and R. Verzicco, J. Fluid Mech. **557**, 307 (2006).
[18] P.-E. Roche, B. Castaing, B. Chabaud, and B. Hébral, Phys. Rev. E **63**, 045303(R) (2001).
[19] X.-L. Qiu, K.-Q. Xia, and P. Tong, J. Turbul. **6**, N30 (2005).
[20] J. C. Tisserand, M. Creyssels, Y. Gasteuil, H. Pabiou, M. Gibert, B. Castaing, and F. Chillà, Phys. Fluids **23**, 015105 (2011).
[21] P. Wei, T.-S. Chan, R. Ni, X.-Z. Zhao, and K.-Q. Xia, J. Fluid Mech. **740**, 28 (2014).
[22] J. Salort, O. Liot, E. Rusaouen, F. Seychelles, J. C. Tisserand, M. Creyssels, B. Castaing, and F. Chillà, Phys. Fluids **26**, 015112 (2014).
[23] S. Wagner and O. Shishkina, J. Fluid Mech. **763**, 109 (2015).
[24] S. Toppaladoddi, S. Succi, and J. S. Wettlaufer, Phys. Rev. Lett. **118**, 074503 (2017).
[25] Y.-C. Xie and K.-Q. Xia, J. Fluid Mech. **825**, 573 (2017).
[26] Y. Shen, P. Tong, and K.-Q. Xia, Phys. Rev. Lett. **76**, 908 (1996).
[27] Y.-B. Du and P. Tong, J. Fluid Mech. **407**, 57 (2000).
[28] O. Shishkina and C. Wagner, J. Fluid Mech. **686**, 568 (2011).
[29] J. Schmalzl, M. Breuer, S. Wessling, and U. Hansen, Europhys. Lett. **67**, 390 (2004).
[30] E. P. van der Poel, R. J. A. M. Stevens, and D. Lohse, J. Fluid Mech. **736**, 177 (2013).
[31] L. N. Howard, J. Fluid Mech. **17**, 405 (1963).
[32] C. R. Doering and P. Constantin, Phys. Rev. E **53**, 5957 (1996).
[33] J. P. Whitehead and C. R. Doering, Phys. Rev. Lett. **106**, 244501 (2011).
[34] B. Castaing, G. Gunaratne, F. Heslot, L. Kadanoff, A. Libchaber, S. Thomae, X.-Z. Wu, S. Zaleski, and G. Zanetti, J. Fluid Mech. **204**, 1 (1989).
[35] D. Goluskin and C. R. Doering, J. Fluid Mech. **804**, 370 (2016).
[36] R. Verzicco and P. Orlandi, J. Comput. Phys. **123**, 402 (1996).
[37] E. P. van der Poel, R. Ostilla-Mónico, J. Donners, and R. Verzicco, Comput. Fluids **116**, 10 (2015).
[38] E. A. Fadlun, R. Verzicco, P. Orlandi, and J. Mohd-Yusof, J. Comput. Phys. **161**, 35 (2000).
[39] H. Johnston and C. R. Doering, Phys. Rev. Lett. **102**, 064501 (2009).
[40] E. P. van der Poel, R. Ostilla-Mónico, R. Verzicco, and D. Lohse, Phys. Rev. E **90**, 013017 (2014).
[41] S. Toppaladoddi, S. Succi, and J. S. Wettlaufer, Europhys. Lett. **111**, 44005 (2015).
[42] X. Zhu, R. Ostilla-Mónico, R. Verzicco, and D. Lohse, J. Fluid Mech. **794**, 746 (2016).
[43] B. Eckhardt, S. Grossmann, and D. Lohse, J. Fluid Mech. **581**, 221 (2007).
[44] D. P. M. van Gils, S. G. Huisman, G.-W. Bruggert, C. Sun, and D. Lohse, Phys. Rev. Lett. **106**, 024502 (2011).
[45] S. Grossmann, D. Lohse, and C. Sun, Annu. Rev. Fluid Mech. **48**, 53 (2016).
[46] P. R. Owen and W. R. Thomson, J. Fluid Mech. **15**, 321 (1963).